N. Bugdayci

D. B. Bogy

F. E. Talke

Axisymmetric Motion of Radially Polarized Piezoelectric Cylinders Used in Ink Jet Printing

An analysis of the low frequency response of piezoelectric squeeze tubes used in drop-on-demand ink jet printing is carried out. The displacements at inner and outer boundaries are determined as a function of voltage and fluid pressure. The results are used to obtain fluid pressure per applied voltage as a function of inner and outer radius. Numerical computations are carried out for PZT-5H, and results are presented in graphical form which can be used to optimize design dimensions. The effect of finite electrode thickness is also studied.

1. Introduction

This study was carried out for the purpose of determining the motion of piezoelectric cylinders used in drop-on-demand ink jet printing technology as described by Zoltan [1]. A cylinder of this kind is typically made of a strongly coupled piezoelectric ceramic that is polarized in the radial direction. The cylinder has a concentric cylindrical hole which is filled with a fluid (ink) during operation. The inner and outer cylindrical boundaries of the ceramic are coated with thin electrodes and are thus constrained to be electrical equipotential surfaces. The ejection of drops results from the interaction of pressure waves due to the radial motion of the cylinder with the free meniscus surface. This motion is produced by the application of an electric potential difference between the two electrodes.

From the general description of the problem given above, it is apparent that a first analysis should emphasize the radial motion of the cylinder. Depending on the specific mounting design, the axial motion may, by assumption, be ruled out or it may be allowed only as incidental to and as a by-product of the radial motion. In the former case, we have a state of plain strain and in the latter case, where we make the assumption of vanishing normal stress in the axial direction, the state is closer to plane stress.

Lazutkin and Tsyganov [2] considered the axisymmetric, plane stress, harmonic radial vibrations of thick-walled short cylinders (rings) and obtained an exact expression for the amplitude of the radial displacement as a function of radial coordinate and frequency. They also calculated the values of the two lowest open-circuit mechanical resonance frequencies. However, their work was restricted to the case of stress-free inner and outer boundaries. Burt [3] extended the solution for the radial displacement in [2] to the case of vanishing frequency (static case). But, in attempting to further extend the solution of [2] to obtain the voltage response to harmonic excitation by internal pressure, he introduced an artificial mechanical condition to determine an unknown electrical parameter despite the fact that a circuit equation is required for that determination. Adelman, Stavsky, and Segal [4] obtained solutions for various boundary conditions in the plane strain case for axisymmetric harmonic radial vibrations.

In this paper we restrict the study to the quasistatic motion of piezoelectric cylinders. For the static case only, the plane stress idealization and other assumptions made in obtaining the deformation of a ring are also adequate for a long cylinder. We also carry out numerical calculations with the

© Copyright 1983 by International Business Machines Corporation. Copying in printed form for private use is permitted without payment of royalty provided that (1) each reproduction is done without alteration and (2) the Journal reference and IBM copyright notice are included on the first page. The title and abstract, but no other portions, of this paper may be copied or distributed royalty free without further permission by computer-based and other information-service systems. Permission to republish any other portion of this paper must be obtained from the Editor.

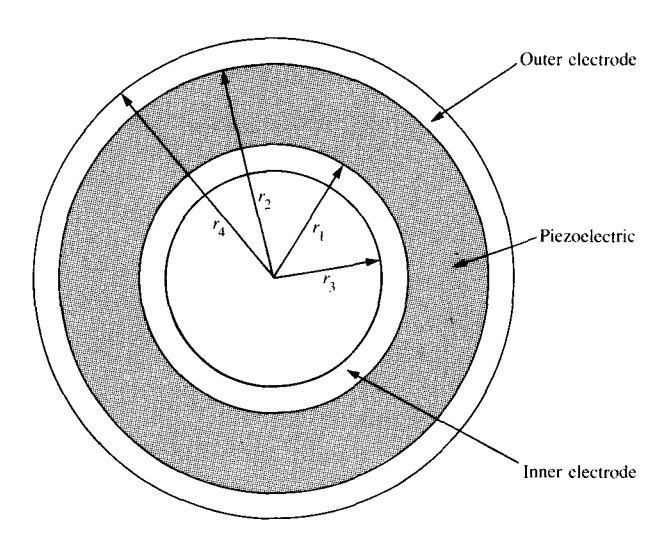


Figure 1 Cross section of piezoelectric cylinder used in ink jet printing.

static solution to predict the response of the squeeze tubes to voltage and pressure excitations at low frequencies. In addition, the mechanical effect of the electrodes on the response of the cylinder is determined. Finally, the question of the optimal cylinder dimensions from the point of view of ink jet application is considered.

2. Theoretical background

The problem is analyzed in terms of the three-dimensional linear theory of piezoelectricity. This theory can be summarized by the following system of 22 field equations in 22 variables that are functions of time t and position (x_1, x_2, x_3) as determined with respect to a Cartesian system of coordinates:

$$T_{ij,i} = \rho \ddot{u}_j, \tag{1}$$

$$D_{i,i} = 0, (2)$$

$$S_{ij} = S_{ijkl}T_{kl} + g_{kij}D_k, (3)$$

$$E_i = -g_{ikl}T_{kl} + \beta_{ii}D_i, (4)$$

$$S_{k\ell} = \frac{1}{2} (u_{k,\ell} + u_{\ell,k}),$$
 (5)

$$E_k = -\phi_{\cdot k}. \tag{6}$$

The lower case latin indices range over 1, 2, 3; summation of repeated indices is implied; a comma denotes partial differentiation, and a superposed dot indicates differentiation with respect to time.

The terms that appear in these equations are Cartesian components of tensors as listed below:

 T_{ii} stress tensor,

D_i electric displacement vector,

 S_{ii} strain tensor,

 E_i electric field intensity vector,

u, displacement vector,

 ϕ electric scalar potential,

 ρ mass density,

 s_{iikl} elastic material tensor,

 g_{ikl} piezoelectric material tensor,

 β_{ii} dielectric material tensor.

We assume that the material is homogeneous, in which case ρ , s_{ijkl} , g_{ikl} , and β_{ij} are constant.

Equations (1) are the local stress equations of motion in the absence of body forces. The condition (2) on the electric displacement vector involves the assumption of a quasistatic electric field. Equations (3) and (4) are the constitutive equations relating strain and electric field intensity to stress and electric displacement. Through the material constants, these equations characterize the behavior of the piezoelectric material. Finally, Eqs. (5) and (6) give the definitions of the mechanical strain and the electric field intensity in terms of the mechanical displacement components and the electric potential, respectively.

It is convenient to express the constitutive relations (3) and (4) in the usual compressed subscript notation:

$$S_I = s_{II} T_I + g_{II} D_I, \tag{7}$$

$$E_i = -g_{ij}\hat{T}_j + \beta_{ii}D_i. \tag{8}$$

In (7) and (8), capital Latin indices have replaced pairs of lower case Latin indices. Accordingly, these capital indices take values 1 to 6.

The behavior of the piezoelectric material can also be characterized by the following alternate set of constitutive equations, which have the mechanical strain tensor and the electric field intensity vector as independent variables:

$$T_I = c_{II} S_J - e_{iI} E_i, (9)$$

$$D_i = e_{ii}S_i + \epsilon_{ii}E_i, \tag{10}$$

where this time c_{IJ} , e_{IJ} , and ϵ_{ij} are elastic, piezoelectric, and dielectric material constants, respectively.

3. Analysis of the problem

We now apply the theory of piezoelectricity summarized above to the problem of determining the response of a hollow piezoelectric cylinder to voltage and pressure excitations. Figure 1 shows the cross section of the cylinder. The inner and outer radii of the piezoelectric layer, the inner radius of the inner electrode, and the outer radius of the outer electrode are denoted by r_1 , r_2 , r_3 , and r_4 , respectively. Figure 2 shows the perspective view of the cylinder along with a cylindrical polar coordinate system. Also shown in this figure is the driving circuit that includes a voltage source. In the analysis that follows we use Eqs. (1)-(10) in their equivalent polar form whenever it is necessary.

The piezoelectric material we are interested in is PZT-5H. This ceramic effectively has the symmetry of a hexagonal crystal in class C_{6v} (or 6mm). The restrictions on the elastic, piezoelectric, and dielectric constants of a material possessing this symmetry are expressed by the following arrays, in which the direction of the x_2 axis of the Cartesian coordinate system is taken to coincide with the direction of polarization:

$$[c_{IJ}] = \begin{bmatrix} c_{11} & c_{12} & c_{13} & 0 & 0 & 0 \\ c_{12} & c_{22} & c_{12} & 0 & 0 & 0 \\ c_{13} & c_{12} & c_{11} & 0 & 0 & 0 \\ 0 & 0 & 0 & c_{44} & 0 & 0 \\ 0 & 0 & 0 & 0 & c_{55} & 0 \\ 0 & 0 & 0 & 0 & 0 & c_{44} \end{bmatrix},$$

$$c_{55} = \frac{1}{2} (c_{11} - c_{13}),$$

$$[e_{ij}] = \begin{bmatrix} 0 & 0 & 0 & 0 & 0 & e_{16} \\ e_{21} & e_{22} & e_{21} & 0 & 0 & 0 \\ 0 & 0 & 0 & e_{16} & 0 & 0 \end{bmatrix},$$

$$[\epsilon_{ij}] = \begin{bmatrix} \epsilon_{11} & 0 & 0 \\ 0 & \epsilon_{22} & 0 \\ 0 & 0 & 0 \end{bmatrix}.$$
(11)

The alternate set of constants s_{ij} , g_{ij} , and β_{ij} also exhibit the same symmetries as those expressed by the above arrays.

The analytical results derived in this paper hold for all piezoelectric materials in class C_{6v} , even though the specific material constant values for PZT-5H are used in the numerical calculations.

The assumptions of the analysis are the following:

1. The motion of the cylinder is axisymmetric. Associated with this assumption are (a) the absence of dependence of field variables on the circumferential coordinate θ and (b) the vanishing of the circumferential displacement u_a .

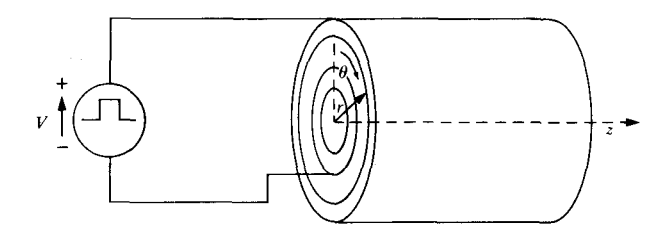


Figure 2 Coordinate system of piezoelectric cylinder and schematic of driving circuit.

- 2. In order to avoid the complications resulting from coupling with the axial modes of motion, we make the assumptions that the radial displacement u_r , and the scalar electric potential ϕ do not depend on the axial coordinate z and also that the axial displacement u_z does not depend on the radial coordinate r.
- 3. We assume the condition of plane stress, i.e., the normal stress in the axial direction is zero. The shearing stress components vanish due to the kinematical assumptions 1 and 2 and the constitutive equations for the piezoelectric ceramic.
- 4. With assumption 3, we can satisfy the equation of motion for the axial direction only in the static case. Physically, this is associated with the fact that axial resonance can result from electrical or pressure excitation in the radial direction. But, for frequencies that are small in comparison with the axial resonance frequency, the cylinder may be assumed to behave quasistatically. We restrict the analysis to such low frequencies and use the static solution in studying the deformation of the cylinders.

In order to obtain an estimate of the frequency range of validity of the analysis to be presented, we derive next the lowest axial resonance by considering one-dimensional wave propagation for a cylinder of length ℓ .

Starting with the kinematical assumptions,

$$u_r = u_\theta = 0; \quad u_z = u_z(z,t); \quad \phi = 0,$$
 (12)

constitutive Eqs. (9) and (10) with arrays (11) yield the following nonvanishing stress and electric displacement components:

$$T_{\theta\theta} = c_{13}u_{z,z}; \quad T_{rr} = c_{12}u_{z,z},$$

$$T_{zz} = c_{11}u_{z,z}; \quad D_r = e_{21}u_{z,z}.$$
(13)

When (13) are substituted into the polar version of the equations of motion (1), we obtain

$$\frac{T_{rr} - T_{\theta\theta}}{r} = 0,$$

 $\frac{\partial T_{zz}}{\partial z} = \rho \ddot{u}_z. \tag{14}$

The circumferential equation of motion and the charge equation are trivially satisfied. For this initial estimate, we can consider the first of (14) as essentially satisfied, since c_{12} and c_{13} are almost equal. (For PZT-5H, the difference is less than 5% of the material constant values.) For harmonic time dependence, the second of (14) gives with Eq. (13)

$$u_{z,zz} + \frac{\rho \omega^2}{c_{11}} u_z = 0, {15}$$

where u_z now stands for the amplitude of the displacement in the axial direction, ρ is the density, and ω is the radial frequency. With the boundary conditions,

$$T_{zz} = 0 \text{ at } z = 0, \ell,$$
 (16)

the natural frequencies of vibration are found to be

$$f_n = \frac{n}{2\ell} \sqrt{\frac{c_{11}}{\rho}} \qquad n = 1, 2, \cdots.$$
 (17)

For a PZT-5H cylinder with $\ell=25$ mm the lowest natural frequency of vibration in the axial direction is calculated to be 81 kHz. Therefore, in such a cylinder, the analysis that follows can be expected to be valid for frequencies that are small in comparison with that value.

Using assumptions 1 and 4 the mechanical polar displacement components and the electric potential can be represented by the following functions:

$$u_r = u_r(r); \quad u_\theta = 0; \quad u_z = u_z(z); \quad \phi = \phi(r).$$
 (18)

The mechanical strain tensor and electric field intensity vector components then become

$$S_{rr} = u_{r,r}; \quad S_{\theta\theta} = \frac{u_r}{r}; \quad S_{zz} = u_{z,z},$$

$$S_{r\theta} = S_{rz} = S_{\theta z} = 0,$$

$$E_{\theta} = E_z = 0; \quad E_r = -\phi_r.$$
(19)

Establishing a local correspondence between the polar θ , r, and z axes and the Cartesian x_1 , x_2 , and x_3 axes, respectively, and substituting (19) in constitutive Eqs. (9) and (10) with the use of arrays in (11), we obtain

$$T_{r\theta} = T_{\theta z} = T_{rz} = 0,$$
 (20)

We also recall here assumption 3:

$$T_{zz} = 0. (21)$$

Now, we substitute Eqs. (20) and (21) into constitutive Eqs. (7) and (8) to produce the following relations:

$$S_{\theta\theta} = s_{11}T_{\theta\theta} + s_{12}T_{rr} + g_{21}D_{r},$$

$$S_{rr} = s_{12}T_{\theta\theta} + s_{22}T_{rr} + g_{22}D_{r},$$

$$S_{zz} = s_{13}T_{\theta\theta} + s_{12}T_{rr} + g_{21}D_{r},$$

$$E_{\star} = -g_{21}T_{\theta\theta} - g_{22}T_{\mu} + \beta_{22}D_{\star}. \tag{22}$$

We also note that a simple expression can be derived for D_r by inspecting the polar cylindrical version of Eq. (2) and using the last two of Eqs. (20) and also the fact that D_r is independent of the θ -coordinate, i.e.,

$$D_r = D_0/r, (23)$$

where D_0 is a constant. We now derive stress-displacement type relations for T_{rr} and $T_{\theta\theta}$ by solving the first two of (22) for these variables and substituting expressions from Eqs. (19) for S_{rr} and $S_{\theta\theta}$ and Eq. (23) for D_r .

$$\Delta T_{\theta\theta} = s_{22}(u_r - g_{21}D_0)/r - s_{12}(u_{r,r} - g_{22}D_0/r),$$

$$\Delta T_{rr} = -s_{12}(u_r - g_{21}D_0)/r + s_{11}(u_{r,r} - g_{22}D_0/r),$$
(24)

where

$$\Delta = s_{11}s_{22} - s_{12}^2. \tag{25}$$

With assumptions (1) to (4) and results (20), the polar form of the stress equations of motion (1) give the following stress equation of equilibrium in the radial direction:

$$\frac{dT_{rr}}{dr} + \frac{T_{rr} - T_{\theta\theta}}{r} = 0. \tag{26}$$

We obtain the radial displacement equation of equilibrium by substituting (24) and (25) into (26):

$$u_{r,r} + \frac{1}{r} u_{r,r} - \frac{\nu^2}{r^2} u_r^{\prime} = \frac{A}{r^2}, \tag{27}$$

where

$$\nu^{2} = s_{22}/s_{11},$$

$$A = (g_{22}s_{12} - s_{22}g_{21})D_{0}/s_{11}.$$
(28)

Equation (27) has the following solution:

$$u_r = c_1 r^{\nu} + c_2 r^{-\nu} - \frac{A}{\nu^2}. \tag{29}$$

The constants c_1 , c_2 , and D_0 are to be determined from the mechanical boundary conditions and the driving circuit equation. The mechanical boundary conditions consist of the specification of the pressure at the cylindrical boundary surfaces:

$$T_{rr}(r_2) = -p_2,$$
 (30)
 $T_{rr}(r_1) = -p_1.$

In (30) p_1 and p_2 are the pressures on the inside and outside surfaces, respectively. The equivalent conditions on the radial displacement at the cylindrical boundaries are obtained by substituting the second of (24) into (30):

$$u_{r,r} - \frac{s_{12}}{s_{11}} \frac{u_r}{r} - \frac{B}{r} = \begin{cases} \frac{-\Delta p_1}{s_{11}} \text{ at } r = r_1\\ \frac{-\Delta p_2}{s_{11}} \text{ at } r = r_2 \end{cases}, \tag{31}$$

where

$$B = \left(g_{22} - g_{21} \frac{s_{12}}{s_{11}}\right) D_0. \tag{32}$$

When the solution (29) is substituted into boundary conditions (31), the following two relations are obtained between constants c_1 , c_2 , and D_0 :

$$c_{1}(\nu + \sigma_{12})r_{\alpha}^{\nu} - c_{2}(\nu - \sigma_{12})r_{\alpha}^{-\nu} - D_{0}s_{\text{eff}}\frac{g_{22}}{s_{22}} = \frac{-\Delta p_{\alpha}r_{\alpha}}{s_{11}}$$

$$\alpha = 1, 2, \qquad (33)$$

where

$$\sigma_{12} = -s_{12}/s_{11},$$

$$s_{\text{eff}} = s_{22} \left(1 - \frac{s_{12}^2}{s_{11}s_{22}} \right).$$
(34)

The third condition needed in the determination of the arbitrary constants of the solution is provided by the voltage equation of the driving circuit shown in Fig. 2. This condition is the specification of the electric potential difference V across the electrodes. We now derive an expression for V in terms of the radial displacement function. From (6), we have

$$V = -\int_{r_1}^{r_2} E_r dr. \tag{35}$$

Substituting (23) and (24) into the fourth of (22) and then using the result in (35), we obtain

$$V = d_1(u_r(r_2) - u_r(r_1)) + d_2 \int_{r_1}^{r_2} \frac{u_r}{r} dr + d_3 D_0 2n \left(\frac{r_2}{r_1}\right),$$
(36)

where

$$d_{1} = (g_{22}s_{11} - g_{21}s_{12})/\Delta,$$

$$d_{2} = (s_{22}g_{21} - s_{12}g_{22})/\Delta,$$

$$d_{3} = [(2s_{12}g_{22}g_{21} - g_{21}^{2}s_{22} - g_{22}^{2}s_{11})/\Delta] - \beta_{22}.$$
(37)

Substitution of the expression (29) into (36) yields

$$c_{1}(r_{2}^{\nu} - r_{1}^{\nu})(d_{1} + d_{2}/\nu) + c_{2}(r_{2}^{-\nu} - r_{1}^{-\nu})(d_{1} - d_{2}/\nu) + D_{0}(d_{3} + d_{2}^{2}\Delta/s_{22})\ln(r_{2}/r_{1}) = V.$$
(38)

The set of three equations (33) and (38) can be solved for the constants c_1 , c_2 , and D_0 to completely determine the static

response. The results can then be substituted into (28) and (29) to yield the displacement u_r . Since we are primarily interested in the motions at the inner and outer surfaces, this displacement function has been evaluated at r_1 and r_2 , and the results are

$$u_{r}(r_{1}) = \alpha_{1}r_{1}p_{1} + \beta_{1}r_{2}p_{2} + \gamma_{1}V,$$

$$u_{r}(r_{2}) = \alpha_{2}r_{1}p_{1} + \beta_{2}r_{2}p_{2} + \gamma_{2}V,$$
(39)

in which the coefficients α_1 , α_2 , β_1 , β_2 , γ_1 , and γ_2 are functions of x, where

$$x = r_1/r_2, \tag{40}$$

as listed below:

$$\begin{split} \alpha_1(x) &= [s_4 x^{-\nu} \ln{(x)} + s_5 x^{\nu} \ln{(x)} + \Gamma_1 x^{\nu} + \Gamma_2 x^{-\nu} \\ &+ \psi]/D(x), \\ \alpha_2(x) &= [-s_6 \ln{(x)} + \Omega_1 x^{\nu} + \Omega_2 x^{-\nu}]/D(x), \\ \beta_1(x) &= [s_6 \ln{(x)} + \Omega_2 x^{\nu} + \Omega_1 x^{-\nu}]/D(x), \\ \beta_2(x) &= [-s_4 x^{\nu} \ln{(x)} - s_5 x^{-\nu} \ln{(x)} + \Gamma_2 x^{\nu} + \Gamma_1 x^{-\nu} \\ &+ \psi]/D(x), \\ \gamma_1(x) &= [\Lambda_1 x^{\nu} - \Lambda_2 x^{-\nu} + \phi]/D(x), \end{split}$$

 $\gamma_2(x) = [\Lambda_2 x'' - \Lambda_1 x^{-r} - \phi]/D(x),$ where the denominator expression D(x) is

$$D(x) = s_{\gamma}(x^{\nu} - x^{-\nu}) \ln(x) + \Phi(x^{\nu} + x^{-\nu} - 2)$$
 (42)

and the constants in (41) are defined as follows:

$$\begin{split} s_4 &= -s_{\rm eff} d_4 \sigma_1 \,, \qquad s_5 &= -s_{\rm eff} d_4 \sigma_2 \,, \\ s_6 &= 2\nu s_{\rm eff} d_4 \,, \qquad s_7 &= \sigma_1 \sigma_2 d_4 \,, \\ \psi &= -4 g_{22} s_{\rm eff}^2 d_2 / \nu s_{22} \,, \qquad \phi = 2 s_{\rm eff} g_{22} / \nu s_{22} \,, \\ \Phi &= 2 g_{22}^2 \, s_{\rm eff} / \nu s_{11} s_{22} \,, \\ \Omega_1 &= -s_{\rm eff}^2 \, (\nu d_1 + d_2) [g_{22} - d_2 (s_{12} - \nu s_{11})] / \nu s_{22} \,, \\ \Omega_2 &= s_{\rm eff}^2 \, (\nu d_1 - d_2) [g_{22} - d_2 (s_{12} - \nu s_{11})] / \nu s_{22} \,, \\ \Lambda_1 &= -s_{\rm eff} \sigma_2 (g_{22} + \sigma_1 d_2 s_{11}) / s_{22} \,, \\ \Lambda_2 &= s_{\rm eff} \sigma_1 (g_{22} - \sigma_2 d_2 s_{11}) / s_{22} \,, \\ \Gamma_1 &= -s_{\rm eff}^2 [g_{22} (\nu d_1 - d_2) \\ &\quad - d_2 (\nu d_1 + d_2) (s_{12} + \nu s_{11})] / \nu s_{22} \,, \\ \Gamma_2 &= -s_{\rm eff}^2 [-g_{22} (\nu d_1 + d_2) \\ &\quad + d_2 (\nu d_1 - d_2) (s_{12} - \nu s_{11})] / \nu s_{22} \,, \end{split}$$

in which

$$\sigma_1 = \nu + \sigma_{12}, \quad \sigma_2 = \nu - \sigma_{12}, \quad d_4 = d_3 + d_2^2 \Delta / s_{22}.$$
 (44)

Many of the numerical results to be presented are for a PZT-5H cylinder with $r_1 = 0.38$ mm and $r_2 = 0.62$ mm. For

(41)

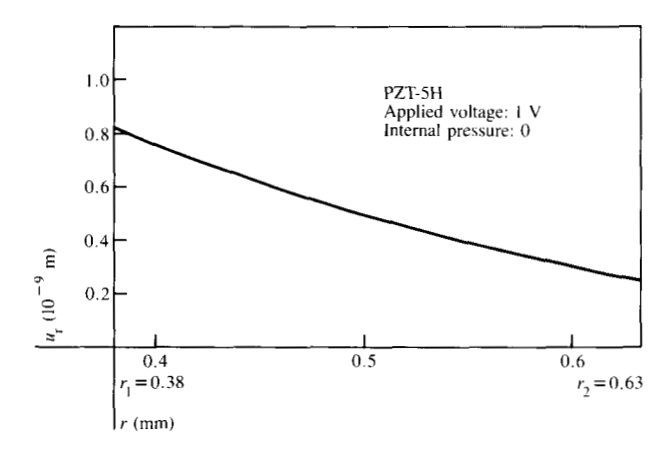


Figure 3 Radial displacement profile across thickness of cylinder.

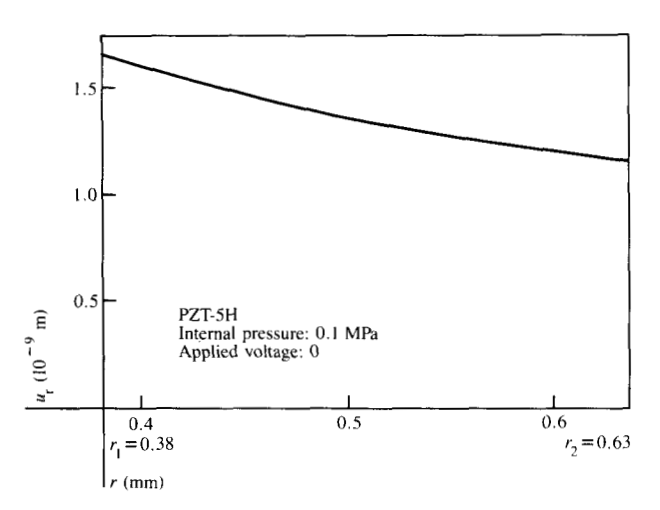


Figure 4 Radial displacement profile across thickness of cylinder.

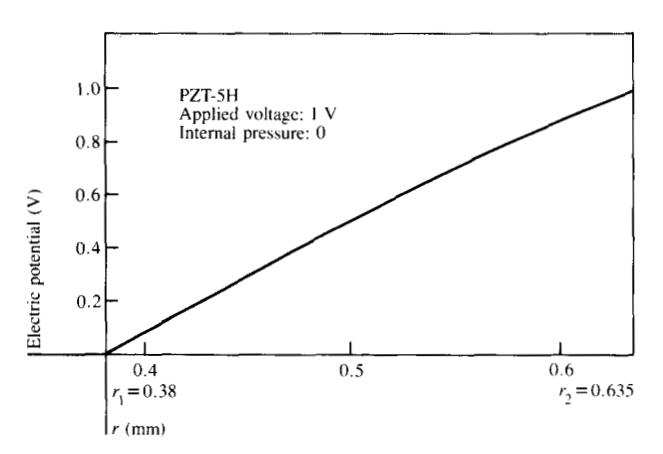


Figure 5 Electrical potential profile across thickness of cylinder.

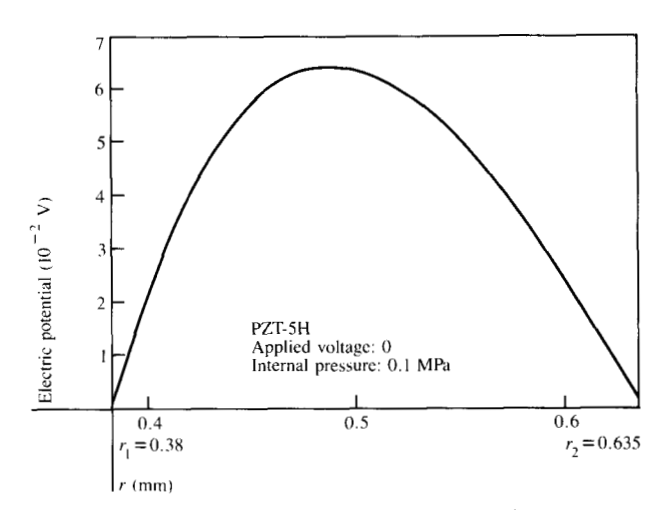


Figure 6 Electrical potential profile across thickness of cylinder.

these parameters the coefficients α_1 , α_2 , β_1 , β_2 , γ_1 , and γ_2 have values as follows:

$$\alpha_1 r_1 = 0.166 \times 10^{-7}, \qquad \alpha_2 r_1 = 0.115 \times 10^{-7},$$

$$\beta_1 r_2 = -0.191 \times 10^{-7}, \qquad \beta_2 r_2 = -0.171 \times 10^{-7}, \qquad (45)$$

with units of m/MPa, and

$$\gamma_1 = 0.815 \times 10^{-9}, \qquad \gamma_2 = 0.240 \times 10^{-9},$$
 (46)

with units of m/volt.

4. Numerical results

Numerical calculations using the static solution were carried out for a PZT-5H cylinder with 0.75 mm inner diameter and 1.25 mm outer diameter. These are typical parameters used, for example, in Zoltan [1]. Figure 3 shows the radial displacement profile across the thickness of a cylinder which has I volt electric potential difference between its electrodes and no pressure on its surfaces. Figure 4 shows the displacement profile across the thickness of a cylinder with shorted electrodes and a pressure of 0.1 MPa applied on its inner surface. Figures 5-10 show the profiles of electric potential, radial stress, and hoop stress across the thickness of the cylinder for both the case in which I volt is applied between the electrodes and no pressure is on the surfaces and the case in which the electrodes are shorted and a pressure of 0.1 MPa is applied on the inner surface. Because of linearity, one can obtain from these graphs the radial dependence of the above variables for arbitrary combinations of applied voltage and internal pressure.

5. Optimization of cylinder dimensions: maximum fluid pressure

Two assumptions were made in the investigation of the

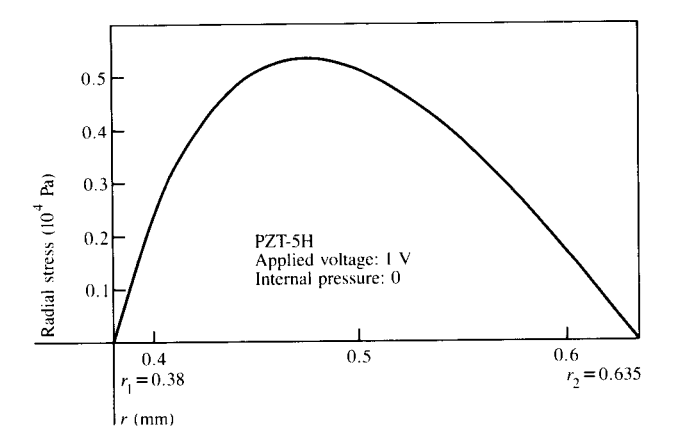


Figure 7 Radial stress profile across thickness of cylinder.

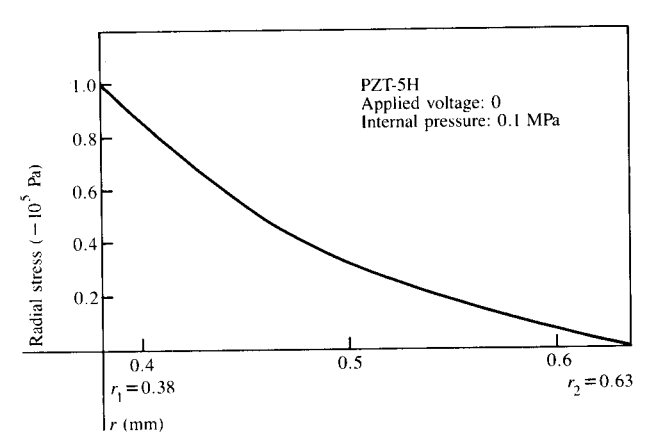


Figure 8 Radial stress profile across thickness of cylinder.

problem of finding the optimal cylinder dimensions for the ink jet application:

- 1. The cylinder was assumed to behave quasistatically.
- 2. The amount of pressure produced in the fluid in a completely enclosed cylinder was used as the criterion of optimization.

If we take for the fluid equation of state,

$$-\frac{dv}{v} = \frac{dp}{B},\tag{47}$$

where v is the volume of the cylindrical cavity filled by the liquid, p is the liquid pressure and B is the liquid bulk modulus, we can, by integrating (47) and expressing the volume change in the cavity in terms of the displacement of the inner surface of the cylinder, arrive at the following result:

$$p = -B\Omega n \left(1 + \frac{2u_r(r_1)}{r_1}\right). \tag{48}$$

Since $u_r(r_1)/r_1 \ll 1$, (48) is approximately equivalent to

$$p = -2Bu_r(r_1)/r_1. (49)$$

The first of (39) gives for the case of no outside pressure on the cylinder,

$$u_{\mathfrak{c}}(r_{\mathfrak{c}}) = \alpha_{\mathfrak{c}} r_{\mathfrak{c}} p + \gamma_{\mathfrak{c}} V, \tag{50}$$

where α_1 and γ_1 are given in Eqs. (40)–(44). Equations (49) and (50) combined yield the following expression for pressure produced per volt applied:

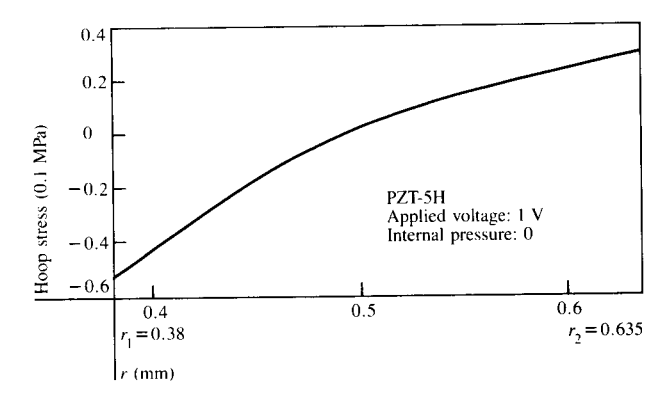


Figure 9 Hoop stress profile across thickness of cylinder.

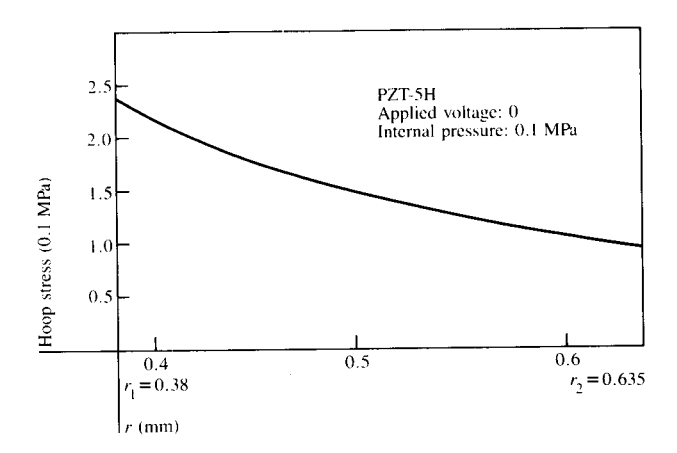


Figure 10 Hoop stress profile across thickness of cylinder.

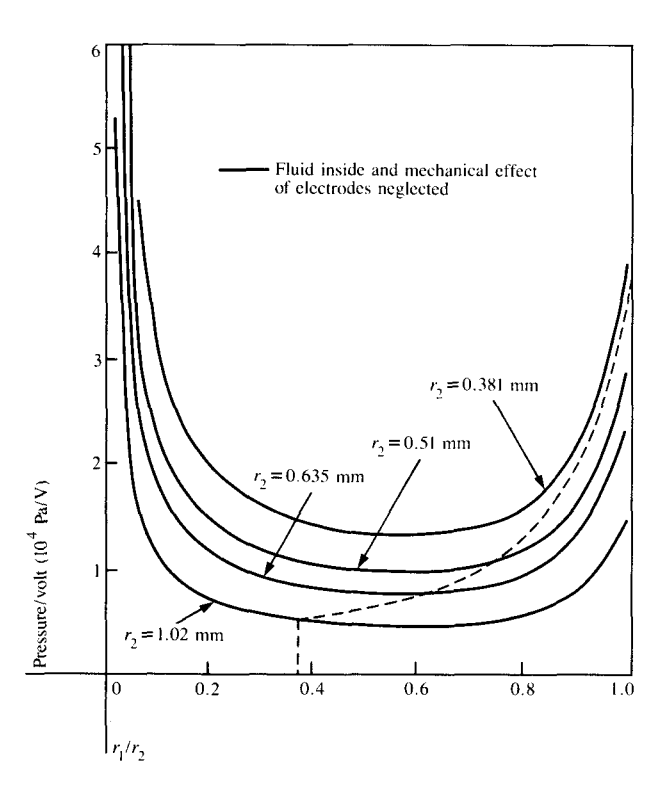


Figure 11 Pressure/volt inside the fluid as a function of r_1/r_2 .

$$p/V = \frac{1}{r_1} \left[\frac{-2B\gamma_1(x)}{1 + 2B\alpha_1(x)} \right]$$

$$= \frac{1}{r_2} \left[\frac{-2B\gamma_1(x)}{x + 2Bx\alpha_1(x)} \right].$$
(51)

In Fig. 11 we show graphs that give the values of this expression for typical values of the inner and outer radii. In the calculations associated with these graphs, the value 2.23×10^3 MPa was used for the bulk modulus B of the liquid. The graphs show that for a fixed ratio of r_1/r_2 the pressure/volt increases as r_2 decreases. This can be seen in (51). For fixed r_2 , we find that p/V is a minimum for r_1/r_2 near 0.6 and increases as r_1/r_2 approaches either zero or one. Neither of these two limiting cases is feasible, since if r_1 is too small, insufficient volume would be available for forming drops, whereas if r_1 approaches r_2 , the critical field strength for depolarization of the piezoelectric tube is exceeded.

In manufacturing piezoelectric cylinders, there is a lower limit on the inside radius for ensuring that a good electrode will be obtained from the plating process. For the case that r_1 is fixed at, say, 0.381 mm, and r_2 is allowed to vary, the dashed curve in Fig. 11 for p/V is obtained. The best design at fixed r_1 is found by choosing r_2 as small as possible without exceeding the safe level of electric field strength. For values of r_1 greater than 0.381, the dashed curve in Fig. 11 is

translated to the right and downward. We therefore conclude that r_1 should be made as small as possible from a manufacturing viewpoint. It should be pointed out, however, that viscous effects in the fluid may invalidate the last conclusion.

6. Optimization of cylinder dimensions: minimum OD displacement

In some designs it may be desirable to have the radial displacement vanish at the outer surface of the piezoelectric cylinder. From (39) it is seen that $u_r(r_2)$ depends on p_1 , p_2 , and V. In order for $u_r(r_2)$ to vanish for arbitrary values of these three forcing functions, it would be necessary for all three of the coefficients α_2 , β_2 , and γ_2 to vanish. It is clear from (41) that these conditions cannot all be met with the same value of x. However, under most conditions the major contribution to the radial motion of the piezoelectric cylinder is the applied voltage, and it is possible to find a ratio r_1/r_2 such that γ_2 vanishes.

The condition for $\gamma_2 = 0$ is obtained from (41) as

$$\Lambda_2 y^2 - \phi y - \Lambda_1 = 0, \tag{52}$$

where

$$y = x'. (53)$$

Solving the quadratic equation (52) and substituting from (43) and (44) the definitions of Λ_1 , Λ_2 , and ϕ , we obtain the two solutions

$$y = 1, \quad (g_{22} + g_{21}\nu)/(g_{22} - g_{21}\nu).$$
 (54)

The first solution yields $x = r_1/r_2 = 1$, and it is not physically meaningful. The second solution yields

$$x = \left(\frac{g_{22} + g_{21}\nu}{g_{22} - g_{21}\nu}\right)^{1/\nu}.$$
 (55)

For PZT-5H cylinders this condition requires

$$x = r_1/r_2 = 0.38. (56)$$

Therefore, if the radial motion of the outside surface of a PZT-5H cylinder is to vanish for any value of applied voltage, in the absence of applied pressures, the ratio of inside to outside radius has to be considerably less than the value $r_1/r_2 = 0.6$ used in the calculations presented in Figs. 3-10.

7. Mechanical effect of electrodes

The mechanical effect of the electrodes on the response of the cylinder has so far been neglected. We now attempt to get an estimate of this effect on the static response, and on the results in the optimization study, by coupling Eqs. (39), which describe the boundary behavior of a piezoelectric cylinder, with the well known solutions [5] for the elastostatic deformation of a hollow isotropic cylinder under internal and external pressure. This solution is summarized

by the following expression for the radial displacement:

$$u_{r}(r) = \frac{1 - \sigma}{E} \frac{a^{2} p_{i} - b^{2} p_{o}}{(b^{2} - a^{2})} r + \frac{1 + \sigma}{E} \frac{a^{2} b^{2} (p_{i} - p_{o})}{(b^{2} - a^{2})} \frac{1}{r},$$
(57)

in which E and σ are Young's modulus and Poisson's ratio, a and b are the inner and outer radii, while p_i and p_o are the inner and outer pressures. In our calculations the following values for pure nickel were used for the material constants of the electrodes:

$$E = 21.6 \times 10^4 \text{ MPa},$$

 $\sigma = 0.31.$ (58)

With some manipulation, (57) can be put into the following form:

$$u_r(r) = h(r;a,b)p_i + h(r;b,a)p_o,$$
 (59)

where the function h is given by

$$h(x;c,d) = \frac{c^2}{E(d^2 - c^2)} \left[(1 + \sigma)x + (1 + \sigma)\frac{d^2}{x} \right].$$
 (60)

Denoting the pressures at radial distances r_1 , r_2 , r_3 , and r_4 by p_1 , p_2 , p_3 , and p_4 , respectively, we apply the result (59) to obtain the two relations,

$$u_{r}(r_{3}) = h(r_{3}; r_{3}, r_{1})p_{3} + h(r_{3}; r_{1}, r_{3})p_{1},$$

$$u_{r}(r_{1}) = h(r_{1}; r_{3}, r_{1})p_{3} + h(r_{1}; r_{1}, r_{3})p_{1}$$
(61)

for the inner electrode; and the two relations,

$$u_r(r_2) = h(r_2; r_2, r_4) p_2 + h(r_2; r_4, r_2) p_4,$$

$$u_r(r_4) = h(r_4; r_2, r_4) p_2 + h(r_4; r_4, r_2) p_4$$
(62)

for the outer electrode.

Next recall from (39) that

$$u_{r}(r_{1}) = \alpha_{1}r_{1}p_{1} + \beta_{1}r_{2}p_{2} + \gamma_{1}V,$$

$$u_{r}(r_{2}) = \alpha_{2}r_{1}p_{1} + \beta_{2}r_{2}p_{2} + \gamma_{2}V,$$
(63)

and from (49),

$$p_3 = -2Bu_r(r_3)/r_3. (64)$$

If V and p_4 are given, the set of equations (61)–(64) constitutes a linear system of seven equations in seven unknowns, $u_r(r_1)$, $u_r(r_2)$, $u_r(r_3)$, $u_r(r_4)$, p_1 , p_2 , and p_3 . Taking $p_4 = 0$ and V = 1 volt, we can solve, in particular, for p_3 to obtain the pressure produced in the liquid per voltage applied between the electrodes. Figure 12 shows three curves giving this pressure as a function of internal radius for a cylinder with outside radius of 0.635 mm. The upper curve shows the results of the analysis in which the mechanical effect of the

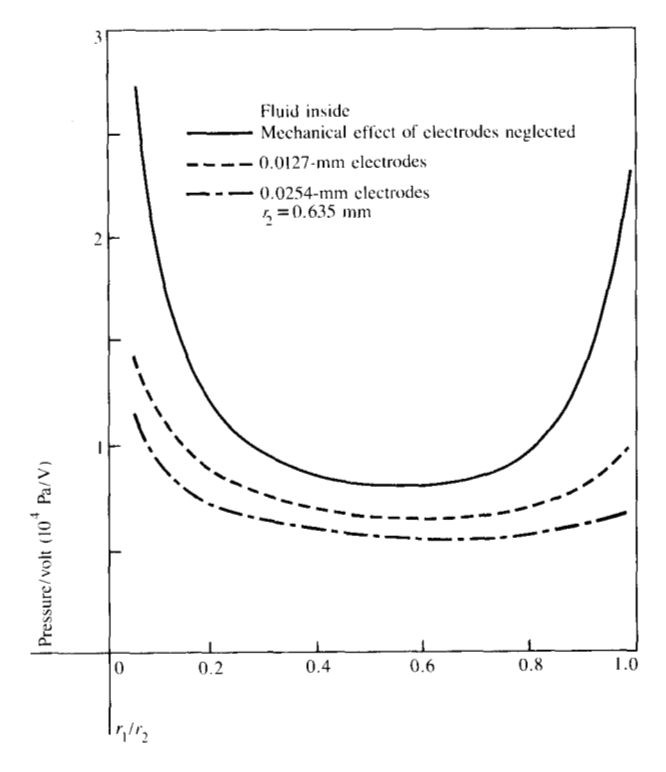


Figure 12 Pressure/volt inside the fluid for different thickness electrodes as a function of r_1/r_2 .

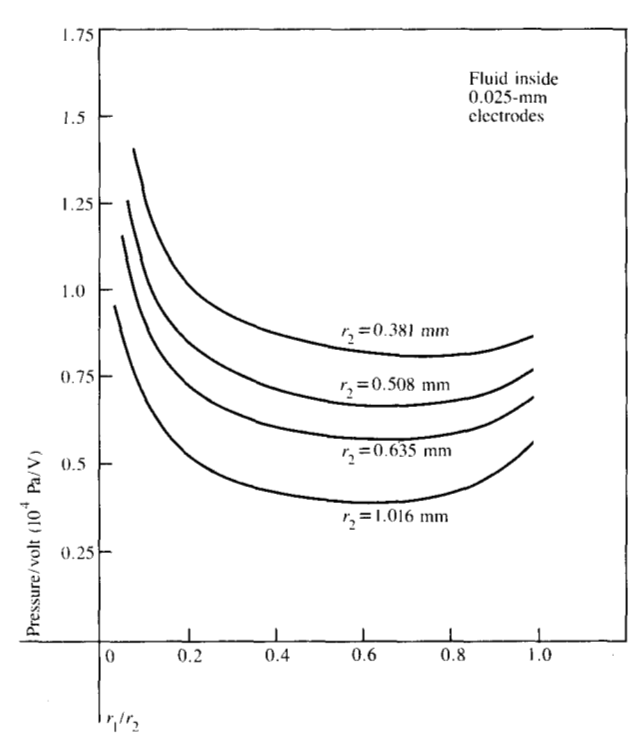


Figure 13 Pressure/volt inside the fluid as a function of r_1/r_2 (electrode thickness = 0.025 mm).

electrodes was neglected, while the lower curves show the results in cases where the mechanical effects of electrodes of 0.0125 mm and 0.0250 mm thickness were taken into account. Comparison of these three curves shows that the pressure is reduced considerably due to the presence of the electrodes. The curves in Fig. 13 correspond to those in Fig. 11 except that in this case the mechanical effect of 0.025-mm-thick electrodes was included in the analysis. The earlier conclusion, that the smaller the outside radius the more pressure is produced for the same amount of voltage applied, still holds true, even though the absolute values for the pressures are lower when the electrodes are taken into account.

8. Summary

Using the axisymmetric quasistatic solution for the motion of radially polarized hollow piezoelectric cylinders, we were able to make certain predictions on the low frequency behavior of squeeze tubes used in ink jet printing technology. Of particular interest was the finding that for a cylinder of typical dimensions the magnitude of the displacement of the inner surface in deformation caused by a voltage difference between the electrodes was more than three times the magnitude of the displacement of the outer surface. Since the outer surface is the only one accessible for experimental measurements, whereas it is the motion of the inner surface that drives the fluid, the importance of this result in the interpretation of experimental data is evident.

In the investigation of the question of optimal cylinder dimensions, it was found that the smaller the cylinder, i.e., the smaller its outer radius, the more fluid pressure was produced per unit voltage applied. When the mechanical effects of the electrodes were taken into account, this result still held true, but the fluid pressure was less sensitive to the value of the inner radius, depending on the thickness of the electrode. The obvious implication of these results for the design of the squeeze tubes used in drop-on-demand ink jet printing is that, in order to reduce the voltage requirements for the printers, the tubes should be made as small as practicable. However, problems with volume supply of ink and clogging of the tubes can be expected to arise if this prescription is followed to the extreme.

References

- S. I. Zoltan, "Pulsed Droplet Ejection System," U.S. Patent 3,902,083, August 1975.
- 2. V. N. Lazutkin and Yu. V. Tsyganov, "Axisymmetric Modes and Electrical Impedance of Radially Polarized Piezoelectric Ceramic Rings," Sov. Phys.-Acoust. 17, 4, 330-334 (1972).
- 3. J. A. Burt, "The Electroacoustic Sensitivity of Radially Polarized Ceramic Cylinders as a Function of Frequency," J. Acoust. Soc. Amer. 64, 6, 1640-1644 (1978).
- N. T. Adelman, Y. Stavsky, and E. Segal, "Axisymmetric Vibrations of Radially Polarized Piezoelectric Ceramic Cylinders," J. Sound Vibration 38, 2, 245-254 (1975).
- S. Timeshenko, Strength of Materials, Part II, D. Van Nostrand Co., Inc., Princeton, NJ, p. 210.

Received September 20, 1982; revised October 28, 1982

David B. Bogy Department of Mechanical Engineering, University of California, Berkeley, California 94720. Dr. Bogy is a Professor of Applied Mechanics at Berkeley and since 1972 has been a consultant to the applied technology group at the IBM Research laboratory in San Jose. His current technical interests include work in anisotropic elastic composites and various types of contact problems on elastic media. He received a B.A. in geology and mechanical engineering and an M.S. in mechanical engineering in 1959 and 1961, both from Rice University, Houston, Texas, and a Ph.D. in applied mathematics in 1966 from Brown University, Providence, Rhode Island. After postdoctoral work in elasticity at the California Institute of Technology, he joined the faculty of the University of California at Berkeley in 1967. Dr. Bogy is a member of the American Society of Mechanical Engineers and Sigma Xi.

Nur Bugdayci University of California, Berkeley, California 94720. Dr. Bugdayci is a research assistant at the University of California working on elastic wave interaction with piezoelectric transducers. He was formerly a Visiting Lecturer in the Mechanical Engineering Department of the University of California, Berkeley. He was a postdoctoral fellow at the IBM Research laboratory in San Jose, California. He received his Ph.D. in applied mechanics and his M.S. in mechanical engineering in 1978, both from the University of California, Berkeley, and his B.S. in engineering in 1975 from Swarthmore College, Pennsylvania. Dr. Bugdayci is a member of Sigma Xi and Tau Beta Pi.

Frank E. Talke

1BM Research Division, 5600 Cottle Road, San Jose, California 95193. Dr. Talke joined 1BM in 1969 at the San Jose Research laboratory and is currently manager of a device mechanics group in the applied science complex in San Jose. Prior to his present involvement in ink jet technology, he studied the mechanical aspects of magnetic recording technology. He attended the University of Stuttgart, Germany, where he received a Diplom-Ingenieur degree (M.S.) in mechanical engineering in 1965, and the University of California at Berkeley, where he received a Ph.D. in mechanical engineering in 1968.